Charge-exchange cross sections and beam lifetimes for stored and decelerated bare uranium ions

Th. Stöhlker,[1,2] T. Ludziejewski,[2] H. Reich,[2] F. Bosch,[2] R. W. Dunford,[3] J. Eichler,[4] B. Franzke,[2] C. Kozhuharov,[2] G. Menzel,[2] P. H. Mokler,[2] F. Nolden,[2] P. Rymuza,[5] Z. Stachura,[6] M. Steck,[2] P. Swiat,[7] A. Warczak,[7] and T. Winkler[1]

[1]*Gesellschaft für Schwerionenforschung (GSI), 64220 Darmstadt, Germany*

[2]*Institut für Kernphysik, University of Frankfurt, Frankfurt, Germany*

[3]*Physics Division, Argonne National Laboratory, Argonne, Illinois 60439*

[4]*Bereich Theoretische Physik, Hahn-Meitner-Institut Berlin, 14109 Berlin, Germany and Fachbereich Physik, Freie Universität Berlin, Berlin, Germany*

[5]*Soltan Institute for Nuclear Studies, 05-400 Swierk, Poland*

[6]*Institute of Nuclear Physics, PL-31342 Cracow, Poland*

[7]*Institute of Physics, Jagiellonian University, PL-30059 Cracow, Poland*

(Received 24 February 1998)

Charge-exchange cross sections and beam lifetimes are studied for decelerated bare uranium ions at the ESR storage ring. By deceleration from the initial energy of 358 MeV/u down to various energies as low as 49 MeV/u, i.e., far below the production energy of bare ionic species, the electron pickup cross sections were obtained for collisions with N_2, Ar, CH_4, and Kr gaseous targets. The measured cross sections and beam lifetimes are compared with the theoretical results for radiative and nonradiative electron capture. The present data, along with the theoretical approximations discussed, provide a solid basis for the estimation of beam lifetimes for decelerated bare high-Z ions. Moreover, a normalization procedure is proposed, in which absolute total charge-exchange cross sections are derived by normalizing the simultaneously measured yield of radiative electron capture photons to rigorously calculated relativistic cross sections. This method, along with the unprecedented beam conditions at the ESR storage ring, allows a significant improvement of the accuracy of cross-section data. [S1050-2947(98)03909-2]

PACS number(s): 34.70.+e

I. INTRODUCTION

The current progress in the basic fields of atomic collision and structure research involving highly charged heavy ions is closely related to the application of both advanced ion sources and advanced accelerator techniques. While in the 1980s new frontiers were reached for relativistic collision conditions [1–10], the study of atomic collisions at ultrarelativistic energies has attracted particular attention in the last few years [11–13]. Also, the recent development of storage and electron-cooler rings opened new challenging possibilities for the investigation of dynamics in electron-ion collisions. For atomic collision experiments dealing with high Z projectiles, a quantum jump was achieved with the advent of the relativistic heavy-ion storage ring (ESR) at GSI in Darmstadt. Here, electron cooling guarantees ion beams of unprecedented quality; i.e., this technique provides cooled and intense beams with precisely known energies, charge states, momentum spread, and beam diameters close to 1 mm.

The interaction of these brilliant beams with matter can be uniquely studied with single-collision conditions at the internal gas-jet target where gas densities of about 10^{12} particles/cm^3 are provided [14]. This can be compared with a typical density of a solid-state target of about 10^{21} particles/cm^3. Nevertheless, due to the high-revolution frequency of the ions within the storage ring of about 10^6 s^{-1}, even collision processes with tiny reaction cross sections (0.1 b or smaller) are accessible at the ESR. Most important and in contrast to conventional single-pass experiments in which direct beams from relativistic accelerators are used, no active or passive beam collimation is required at the ESR. Thus, experimental conditions are almost completely background-free.

In this paper a further unique feature of the ESR will be stressed, i.e., the deceleration capability of the storage ring that allowed us to investigate charge-exchange processes for highly charged ions in a completely different energy and charge-state domain. We present results of an experiment performed for stored and decelerated bare uranium ions. Here, electron-capture cross sections were measured in collisions of 49, 68, 220, and 358 MeV/u U^{92+} with N_2, CH_4, Ar, and Kr gaseous targets. The results provide an experimental basis for estimates of beam losses at accelerator facilities exploiting highly charged decelerated heavy ions. Such data are urgently needed, since currently there is special interest in experiments where highly charged ions are decelerated to final energies far below the production energy of such ionic species. Here, a scenario is under discussion in which ions up to bare uranium are decelerated almost to rest in order to be captured in ion traps [15]. The success of these techniques, however, depends in a crucial way on precise knowledge of the charge-exchange processes by an interaction of the ions with the residual gas, leading to beam losses during the deceleration procedure. The latter may drastically reduce the lifetimes of stored ion beams and may constitute the most serious limitation for the experiments under discussion. However, for bare high-Z ions at low energies neither reliable theoretical estimates nor experimental data on total charge-exchange cross sections exist.

Moreover, in this paper, the question of the accuracy of absolute cross-section measurements at the ESR will be ad-

dressed. In order to deduce absolute cross-section values, we normalized the yield of down-charged projectiles to the simultaneously measured x-ray emission of radiative electron capture to the *K* shell of the projectiles (*K*-REC). Here, as will be discussed in detail below, we exploit the fact that differential REC cross sections are known with high precision. This technique, along with the clean experimental conditions at the ESR, should allow for a substantial improvement in the accuracy of absolute cross-section measurements, which in conventional experiments are limited to a typical precision of 20–50 %. Also, this method can be applied to the study of the various dynamic processes occurring in fast ion-atom collisions, such as excitation, ionization, or electron bremsstrahlung. With the improved accuracy even tiny effects, which were, until recently, beyond the scope of standard collision experiments, can now be investigated.

The organization of the paper is as follows. First, the experimental arrangement used is discussed in Sec. II. Then, in Sec. III, the normalization procedure that was used for the determination of total cross-section data is outlined. They are derived from the observation of down-charged U^{91+} ions and of *K*-REC photons detected in coincidence by a photon detector. Doubly differential REC cross sections calculated in the exact relativistic framework were used to normalize the total charge-exchange cross section to the number of *K*-REC events. The experimental cross sections are compared with theoretical results for the nonradiative and the radiative electron-capture process. Thereafter, in Sec. IV, the experimental lifetimes measured for the stored ions are presented and discussed. Finally, in Sec. V, a short summary is given.

II. EXPERIMENT

The study of electron-capture processes by U^{92+} ions was performed at the heavy-ion synchrotron and storage-ring facility (SIS and ESR) at the Gesellschaft für Schwerionenforschung in Darmstadt. The experimental arrangement at the ESR gas target is shown in Fig. 1. Bare uranium ions, delivered by the SIS with an initial energy of 360 MeV/u, were stacked and accumulated in the ESR storage ring. In the electron-cooler device, the ions were cooled by an electron beam of 200 mA providing U^{92+} ions with a relative momentum spread of about 5×10^{-5}. Typically, 10^8 bare uranium ions were stored and cooled, forming a beam with a diameter (full width at half maximum) of 2 mm.

After completion of the cooling cycle, the gas-jet device [14,16] was switched on. N_2, CH_4, Ar, and Kr gaseous targets with densities between 10^{11} and 10^{12} particles/cm^2 were used. The beam energy loss, caused by the interaction of the ions with the gas target, was compensated by the continuously active electron cooler. After the initial accumulation and cooling of the stored ions at 360 MeV/u, the ions were decelerated to the final beam energies of 49, 68, and 220 MeV/u. For this purpose, the electron cooler was switched off and the coasting beam was rebunched and decelerated while simultaneously ramping down the magnetic fields. At this final stage of beam handling the electron cooler was switched on again. By applying this procedure, up to 2×10^7 ions could be decelerated with an efficiency close to 80%. The current of the beam was measured by means of a calibrated current transformer, while the revolution frequency and momentum spread of the stored ions were monitored by means of Schottky noise analysis. At the two lowest beam energies, the electron cooler current was kept at the relatively low value of 50 mA at 68 MeV/u and 20 mA at 49 MeV/u in order to avoid large beam losses by radiative recombination in the cooler section of the ring.

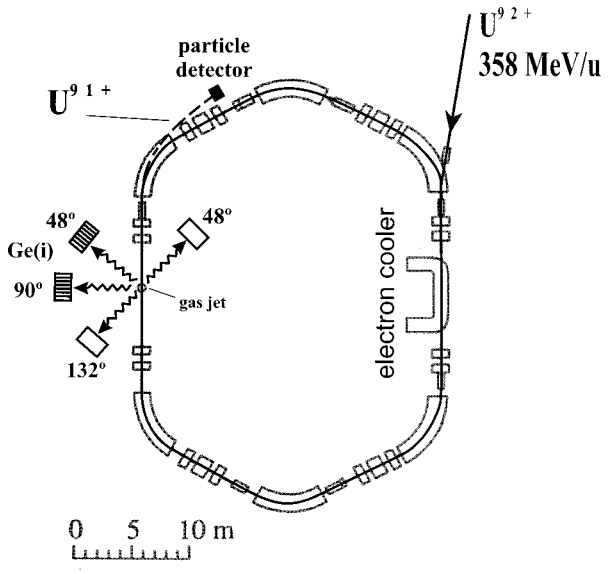

FIG. 1. Schematic diagram of the experimental arrangement at the ESR storage ring. Projectile x rays are registered by four Ge(i) detectors viewing the gas-jet interaction region at angles of 48°, 90°, and 132°. The down-charged U^{91+} ions are separated by a dipole magnet and detected by a fast plastic scintillator counter.

The x rays emitted from the reaction volume were registered by four Ge(i) detectors mounted at observation angles of 48°, 90°, and 132°. The x-ray detector setup was also used for the spectroscopic investigation of the ground-state Lamb shift in H-like uranium. The details of the x-ray detector setup and the spectroscopic data, collected in that experiment, will be presented in a forthcoming paper [17]. Downstream from the reaction region, behind the first dipole magnet, a fast plastic scintillator was located. The detector registered with an efficiency of practically 100% uranium ions, having captured one electron in the reaction region. The x-ray spectra were recorded in coincidence with the down-charged U^{91+} ions. Fast scalers and pulsers were used to correct for possible dead-time effects, and to provide information on the time scale. In principle, pileup corrections must also be considered. Electronic pileup takes place when two events are registered in a time distance shorter than the time resolution of the electronic setup. For the x-ray/particle coincidence measurements, the time resolution is determined by the rise time of the Ge(i) detector signals, which is typically in the range between 50 and 150 ns. However, due to the dc characteristics of the structure of the circulating ion beam and the moderate charge-exchange rates that never exceeded 10^6 s^{-1}, pileup corrections are completely negligible in our experiments at the ESR. Consequently, random events are also most unlikely to occur. They contribute less than 5% to the total number of x-ray–particle coincidence events. For completeness, coincident x-ray spectra were corrected for random events.

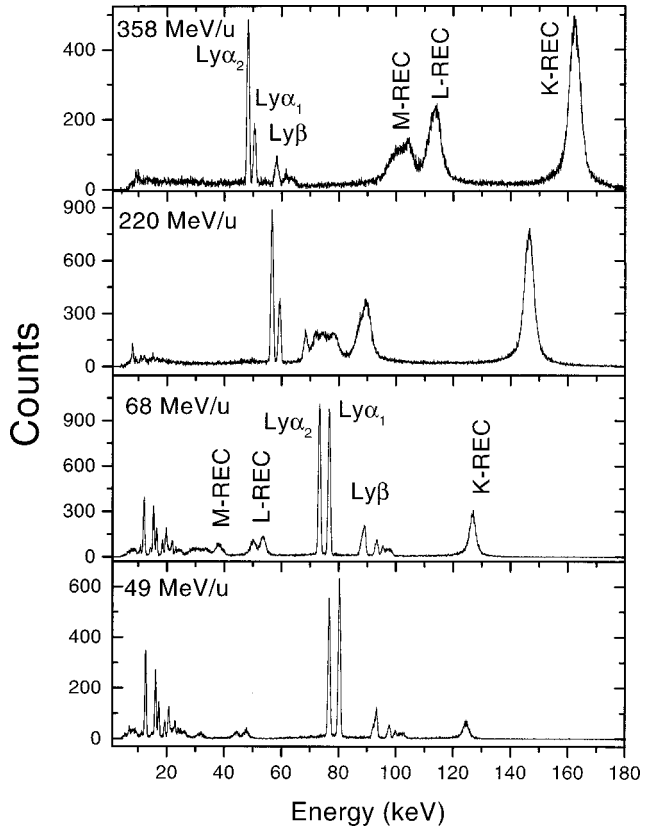

FIG. 2. Typical x-ray spectra registered in coincidence with the particle counter for 49, 68, 220, and 358 MeV/u U^{92+} interacting with N_2 gas targets. The spectra (laboratory frame) were measured at the observation angle of 132° and are not corrected for detection efficiency.

Figure 2 shows examples of x-ray spectra registered at beam energies of 49, 68, 220, and 358 MeV/u by the detector placed at 132° in coincidence with down-charged U^{91+} ions for $U^{92+} \rightarrow N_2$ collisions. The spectra show x-ray radiation corresponding to REC in the empty K and higher shells of the projectile as well as the characteristic Lyman and Balmer lines. Simultaneously, as the projectile energy decreases, the Doppler-shifted characteristic Lyman-$\alpha_{1,2}$ transitions (Lyα_1: $2p_{3/2} \rightarrow 1s_{1/2}$; Ly$\alpha_2$: $2p_{1/2}$, $2s_{1/2} \rightarrow 1s_{1/2}$) become more intense and exhibit a strong change in the relative intensities of the Lyα_1 and Lyα_2 components. These features reveal the energy dependence of the population of excited projectile levels.

III. TOTAL CROSS SECTIONS DERIVED FROM NORMALIZATION TO *K*-REC

A detailed knowledge of the geometry of the beam-target overlap is required in order to measure the absolute cross sections related to charge-exchange processes. Factors such as the gas-target density, as well as the absolute beam intensity, introduce systematic uncertainties, which, for the particular case of experiments at the ESR storage ring, usually amount to about 30% [18]. These uncertainties are removed in the present experiment by an application of the relative normalization method that is discussed in the following. In the proposed approach, the total electron pickup processes are normalized to the number of *K*-REC events registered by an x-ray detector. The electron-capture cross section σ is then given by the expression

$$\sigma = \frac{N^{U^{91+}}}{N^{K\text{-}REC}} \varepsilon \int \frac{d\sigma_K^{REC}}{d\Omega} d\Omega, \tag{1}$$

where $N^{U^{91+}}$ is the number of down-charged U^{91+} ions registered by the particle detector, $d\sigma_K^{REC}(\theta)/d\Omega$ is the theoretical differential cross section for *K*-REC at the angle of observation θ, $N^{K\text{-}REC}$ is the number of *K*-REC photons registered by the x-ray detector, ε is the photon detection efficiency, and $d\Omega$ is the solid angle covered by the x-ray detector. The latter two factors define the overall x-ray detection efficiency and a precise knowledge of their absolute values determines the final experimental accuracy. In our experiments at the ESR gas-jet target, the distance between the x-ray detectors and the gas-jet is in the range between 300 and 400 mm that corresponds, depending on the active area of the detector used, to a solid angle of about $\Delta\Omega/4\pi \approx 10^{-4}$. Therefore, the application of the approximation

$$\int \frac{d\sigma_K^{REC}}{d\Omega} d\Omega \approx \frac{d\sigma_K^{REC}}{d\Omega} \Delta\Omega \tag{2}$$

is justified and does not lead to any significant loss in the accuracy of the normalization procedure. This has been checked by a Monte Carlo simulation taking into account the extended beam-target geometry and the finite angular acceptance of the x-ray detectors used.

Also, the distances between the x-ray detectors and the gas jet are known to a precision of better than 2 mm, which introduces an uncertainty for the solid angle of the x-ray detector of close to 1%. By using sophisticated, laser-assisted measurements of the x-ray/jet-target geometry, used in spectroscopy experiments [19], this value can still be improved and an uncertainty below the 1% level is feasible for solid angle determination. The knowledge of the absolute x-ray detection efficiency depends crucially on the x-ray energy regime of relevance. Typically, for our experiments, the x-ray detection efficiencies are measured by using absolutely calibrated, mixed γ sources, containing γ lines from ^{57}Co, ^{60}Co, ^{241}Am, ^{133}Ba, and ^{169}Yb, where the individual line strengths are known within an absolute accuracy of about 5%. Such calibration sources are well suited for the efficiency determination at energies in the range between 80 keV and 1.5 MeV. For the particular case of planar Ge(i) detectors with thicknesses in the range between 12 and 15 mm (typically used in our experiments) and x-ray energies below 200 keV, the detection efficiency is, in general, close to 50%. The exact value and its related uncertainty depend on the particular x-ray energy and detector used. For the detector placed at a 132° observation angle, where the *K*-REC centroid energy is located close to 160 keV, we estimate conservatively a 5% uncertainty introduced by the efficiency correction. This error determines our overall systematic uncertainty.

Finally, the systematic error that can be introduced by scintillator darkening must be mentioned. It is related to physical damage of the scintillator material at the location of the beam spot, which results in a reduction of the signal

amplitudes and may therefore lead to efficiency losses. If, however, the total electron-capture rate is normalized to the number of x-ray events associated with electron capture, i.e., measured in coincidence with the particle detector, this uncertainty cancels out.

The underlying assumption of this procedure is that *K*-REC cross sections are known to high accuracy. The radiative electron-capture process was observed for the first time in the early 1970s [20–22], and since that time has been extensively studied theoretically [23–28], as well as experimentally, at different collision conditions including heavy projectiles up to bare uranium (see [18], and references therein). Conventionally, REC has been treated as the inverse of the photoelectric effect, leading to the widely applied nonrelativistic dipole approximation [29]. Recently, the theory of REC has been refined and extended up to the relativistic collision regime by incorporating exact relativistic Coulomb wave functions for the bound and the continuum projectile states [26–28]. It has been demonstrated that the results of this relativistic theory are in excellent agreement with experimental *K*-REC cross sections [18] and with subshell-resolved, angular differential cross-section data for high-*Z* ions [30]. Therefore, an application of Eq. (1), in which exact relativistic calculations of *K*-REC cross sections are exploited, seems to be well justified for the determination of charge-exchange cross sections, particularly when dealing with observation angles in the range between 30° and 150° [31]. Here, the theoretical precision should be close to the 1% level. For the case of high-*Z* ions, this restriction to the observation angles quoted is required since a strong influence of spin-flip transitions on the angular distribution is predicted, which should show up most pronounced at observation angles smaller than 30°. Currently, investigations are in progress to confirm this effect experimentally.

A. Analysis of the spectra

For data analysis, the x-ray spectra that are measured in coincidence with the down-charged ions were first energy calibrated and corrected for detection efficiency. The number of counts $N^{K\text{-}REC}$, associated with REC into the *K* shell were obtained by an integration over the *K*-REC spectral distribution. For this purpose theoretical doubly differential cross sections were used for a fit of the experimental *K*-REC line shapes, whereby a linear background was also taken into account. This background, which contributes by less than 5% to the total intensity in the energy regime of relevance for *K*-REC, can be attributed to Compton scattering and to electron bremsstrahlung followed by electron capture into the projectile.

The theoretical double-differential cross sections are derived from exact cross sections for radiative recombination and by adopting the impulse approximation that accounts for the initial binding energy and the momentum distribution of the target electrons (Compton profile). As discussed in detail by Ichihara *et al.* [26], the convolution with the momentum distribution of the electrons in the target atom was done in a rigorous relativistic manner, which takes into account that the effective momentum of the target electron with respect to the projectile does not usually coincide with the beam direction. The momentum distributions are obtained by Fourier-transforming appropriate Roothaan-Hartree-Fock wave functions [26,32]. For the fit of the experimental data, the doubly differential cross sections for capture from all target shells into the *K* shell were calculated and added up. Since, due to the width of the Compton profiles, tails from REC into the *L* and *M* shells may slightly overlap with the *K*-REC distribution, the differential cross sections for all *L* and *M* subshell levels were also considered. Finally, the resulting theoretical REC photon distribution was adjusted to the experimental spectrum by using a one-parameter fit for the spectrum amplitude. The results of this line-shape analysis are depicted in Fig. 3 for the particular cases of the N_2 and Ar targets at 358 MeV/u. The solid line refers to the theoretical spectral shape.

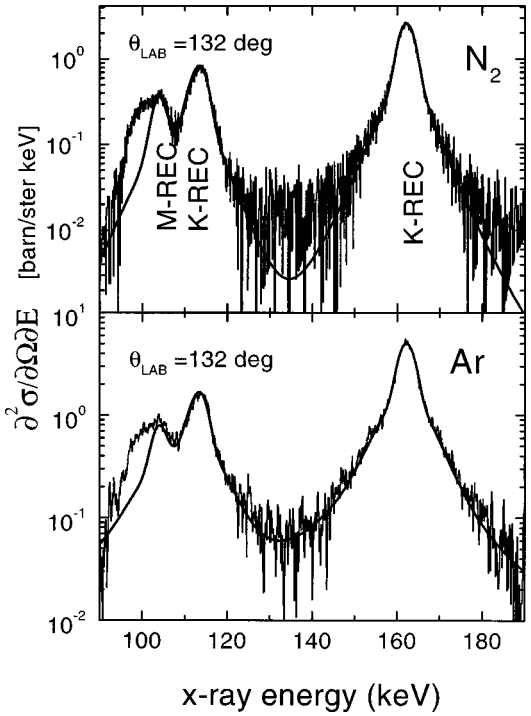

FIG. 3. Theoretical doubly differential REC photon cross sections (solid line) for 358 MeV/u $U^{92+} \rightarrow N_2$ (upper part) and Ar (lower part) collisions in comparison with the experimental data. For comparison, the experimental spectra are adjusted in amplitude to the theoretical results by a least-squares fit.

In the figures, results are shown that were obtained from a least-squares fit of the experimental spectra to the theoretical results. For the *K*-, *L*-, *M*-REC regime considered in the calculation, excellent agreement between the experimental and theoretical spectral distributions is found. Only in the case of the N_2 target are slight deviations observed in the energy regime around 135 keV. Since for the calculation the wave functions of atomic nitrogen were used, we attribute this finding to the difference between the Compton profiles for atomic and molecular nitrogen.

For the case of the Ar target, we show in addition in Fig. 4 a comparison between experiment and theory restricted to the *K*-REC regime. The individual contributions of the Compton profiles of the various target shells are given separately. The agreement between experiment and theory found in the figure illustrates that the rigorous relativistic calculations applied are indeed able to model experimental double-differential REC cross sections precisely.

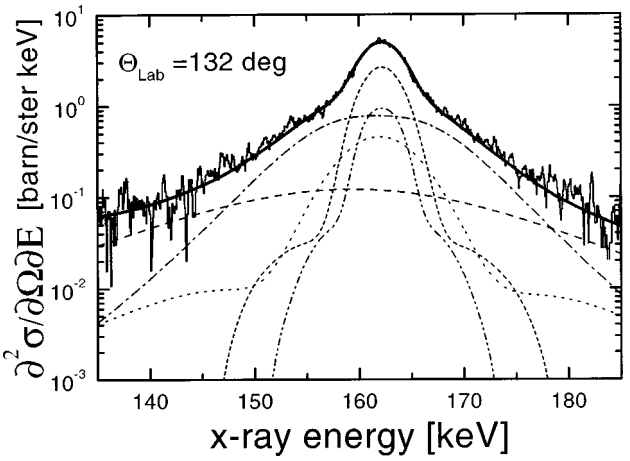

FIG. 4. Same as the lower part of Fig. 3 but restricted to the *K*-REC regime. In addition, the individual contributions from the Compton profiles of the various shells of the Ar target are given separately. $1s$, — — —; $2s$, · · ·; $2p$, · — ·; $3s$, — · · —; $3p$, (· - ·).

B. Results

Figure 5 shows a comparison of the experimental electron-capture cross sections for $U^{92+} \rightarrow N_2$ along with the theoretical predictions for the REC and the nonradiative electron capture (NRC) processes. The errors given arise from the statistical uncertainties in the number of *K*-REC photons and include the systematic uncertainties discussed in the preceding section. For a theoretical description of the NRC process, the eikonal approximation was applied [2,3,6,33]. For details of the calculation we refer to Refs. [33–35].

For the total REC cross sections, nonrelativistic dipole approximation calculations were performed. In general, the results of this simplified approach are in good agreement with both the experimental data and the complete relativistic calculations. Since the latter involves significant contributions from higher multipoles and yields different angular distributions, the agreement with the nonrelativistic dipole approximation must be regarded as fortuitous. See Ref. [18].

In Fig. 5, the total cross-section data are depicted. In addition, we present in the lower part of the figure the relative deviation between the experimental and theoretical results. Here, for the highest beam energies of 220 MeV/u and 358 MeV/u, the results of the complete relativistic calculations for the total cross sections are also shown. The latter can be used as a consistency check for our experimental method. Indeed, an excellent accordance between the complete theory and the experimental findings, deduced from the *K*-REC intensity, can be stated.

For the two lowest beam energies the process of NRC dominates (the importance of NRC at the lowest energies is also manifested by the strongly enhanced intensities of the characteristic Lyman lines as shown in Fig. 2). Here, the results of the theoretical approach applied and the experimental data also coincide with each other. In fact, the eikonal approximation [33,36] reproduces the results of more basic two-center coupled-channel calculations very well [37] and, in general, is found to give a good description of experimental data [6,11]. In Fig. 6, the electron-capture cross sections measured at 220 MeV/u, which were obtained for CH_4, N_2, Ar, and Kr gaseous targets, are shown. In the figure, the data are compared with theoretical cross-section estimates. Here, the NRC and the REC processes were taken into account as discussed above. Again, the experimental results are in moderate agreement with the theoretical approach. However, for the heaviest target Kr where NRC dominates, the applied theoretical approach deviates significantly (within a factor of 2) from the experimental result.

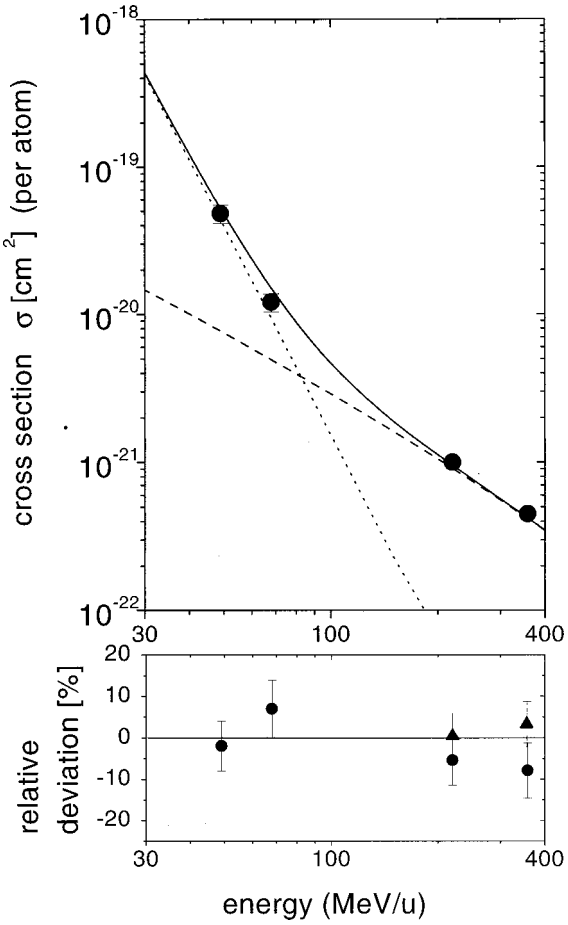

FIG. 5. Total electron-capture cross sections for U^{92+} on a N_2 target versus projectile energy. The dotted line represents the result of the eikonal approach for the NRC process. The dashed line gives the prediction obtained within the dipole approximation for the REC process. The solid line refers to the sum of both predictions. In the lower part of the figure the relative deviation between experiment and theory is depicted, i.e., $(\sigma_{theory}-\sigma_{expt})/\sigma_{theory}$. Here, the solid triangles refer to the cross sections obtained from rigorous relativistic calculations, whereas the full circles refer to the dipole approximation.

To summarize, a good overall agreement is found between the experimental data and the applied theoretical approach. Consequently these findings lend support to the reliability of these approximations for a calculation of cross sections for electron capture into decelerated high-Z ions, as long as the nuclear charge of the target involved in the collision is not too large.

IV. BEAM LIFETIMES

The lifetime of a cooled ion beam in a storage ring is determined by the electron pickup rates of the ions interact-

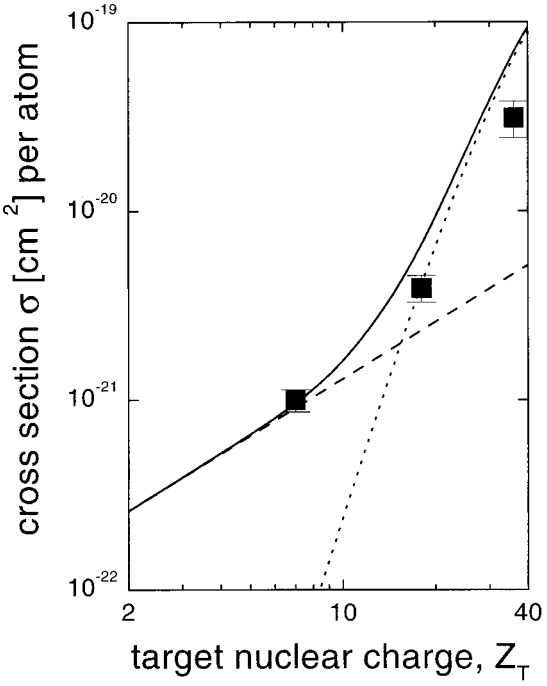

FIG. 6. Target atomic number dependence of the total-electron-capture cross sections for 220-MeV/u U^{92+} interacting with gaseous targets. The theoretical models used are identical to those presented in Fig. 5.

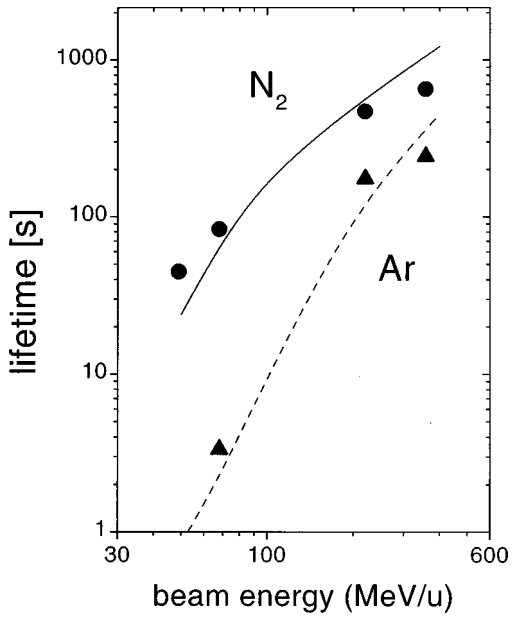

FIG. 7. Experimental lifetimes obtained at the various beam energies for the case of a N_2 (solid points) and an Ar (solid triangle) gaseous target (1×10^{12} particles/cm^2). The solid line and the dashed line (for the N_2 and Ar target, respectively) represent theoretical lifetime estimates (see text).

ing with the residual gas and the radiative recombination rate in the electron cooler. However, if the gas target is used, the lifetime of the beam is essentially determined by electron-capture processes occurring in the gas-jet volume. The cross sections for the latter process is connected to the lifetime of the stored beam by the relation

$$\frac{1}{\tau}=\lambda=\rho\sigma f, \tag{3}$$

where λ denotes the charge-exchange rate, ρ is the thickness of the gas-jet target, and f is the revolution frequency of the circulating ion beam. The number of stored ions, as well as the counting rate of down-charged U^{91+} ions in the particle detector is, therefore, an exponentially decreasing function of time. The lifetimes obtained for the various beam energies are depicted in Fig. 7 for the case of a N_2 and of an Ar gaseous target. In all cases considered the data refer to a target thickness of 10^{12} particles/cm^2. The solid and the dashed lines represent theoretical lifetime predictions (for the N_2 and Ar target, respectively) where both the radiative and the nonradiative electron-capture processes are considered. Here, charge exchange due to the interaction with the residual gas and due to radiative recombination in the cooler section were taken into account. For the loss rate caused by the residual gas, a rough estimate can be obtained by assuming a composition of 79% H_2, 20% N_2, and 1% Ar at a mean pressure of about 10^{-11} mbar.

Although these estimates are rather uncertain (at least within a factor of 2) it turns out that even at the lowest beam energy of 49 MeV/u beam losses due to the residual gas can still be neglected as long as the jet target is used. For the recombination rate in the electron cooler, the Bethe-Salpeter approach [38] was used and a transverse temperature of 0.2 eV was assumed. Depending on the combination of electron-beam current, ion-beam energy and gas-target thickness chosen, recombination in the cooler may contribute considerably to the total beam losses in the ring. In general, however, this process is only of minor importance when the gas-jet target is used. This can be derived from the measured pressure dependence of the beam lifetime, displayed in Fig. 8. The data were obtained for a N_2 target at the energy of 68 MeV/u. The linear increase of the charge-exchange rate with increasing gas-target density (Fig. 8) also provides a consis-

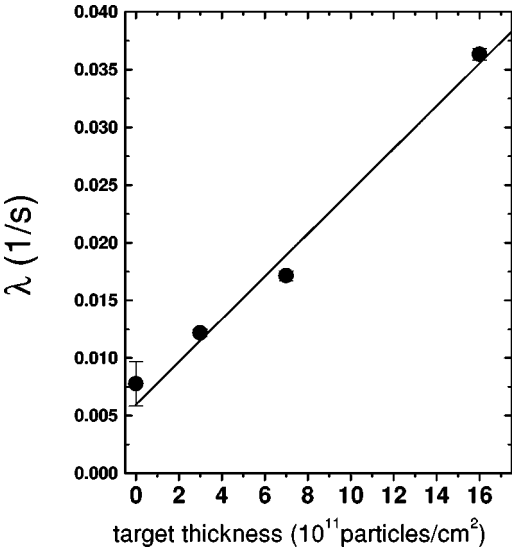

FIG. 8. The dependence of the total charge-exchange rate of a stored U^{92+} beam on the thickness of the N_2 gas-jet target. The data were deduced from lifetime measurements at a beam energy of 68 MeV/u.

TABLE I. Experimental beam lifetimes measured for stored bare uranium ions interacting with the gas-jet target at the ESR storage ring.

Beam energy (MeV/u)	Target	Thickness $P/cm^2 \times 10^{+11}$	Cooler current (mA)	Lifetime (s)
49	N_2	16	20	28
49	CH_4	40	20	57
68	N_2	17	50	49
68	CH_4	17	50	83
68	Ar	5	50	6.7
220	N_2	10	100	468
220	CH_4	48	100	265
220	Ar	9.1	100	192
220	Kr	17	100	33
358	N_2	5	200	1300
358	Ar	2.6	200	931

tency check for the performance of the gas-jet target, i.e., for the relation between the measured gas-jet pressure and the actual gas-jet density.

The estimated theoretical lifetimes in Fig. 7 are in moderate agreement with the experimental data. We attribute this finding to the number of processes and their associated uncertainties, which must be considered when dealing with theoretical lifetime predictions. Also, one has to consider a possible imperfect overlap of the stored beam with the gas-jet volume. Hence, the lifetimes measured directly from the time dependence of the number of particles stored in the ring reflect the effective charge-exchange rates but cannot be used for a precise determination of total charge-exchange cross sections. However, since the measured lifetimes are of importance for experiments dealing with highly charged, decelerated ions we quote in the table representative beam lifetime data measured with various gaseous targets at different beam energies, target densities, and electron-cooler currents.

Finally, it is interesting to estimate, on the basis of the experimental charge-exchange cross sections, the lifetime of the stored ion beams with the gas-jet target switched off. For the particular case of U^{92+} ions at 49 MeV/u, a cooler current of 20 mA was applied and the lifetime was still dominated by radiative recombination in the electron cooler and not by charge exchange in the residual gas. Assuming the composition for the residual gas given above, the calculated loss rate agrees within 30% with the measured one and is about five times smaller than the recombination rate. For the case studied, the storage time (gas jet off) is still of the order of a few minutes. However, for even lower energies, assume for instance 10 MeV/u U^{92+}, the lifetime may drop down to only 5 s without any additional gas target. Here, the heavy components of the residual gas, e.g., Ar, are of particular relevance (compare Table I). In order to determine the feasibility of experiments for such exotic conditions, one has to first establish experimentally the relevant charge-exchange cross sections.

V. SUMMARY

We reported the results of an experiment performed for stored and decelerated bare uranium ions where electron-capture cross sections were measured in collisions of 49, 68, 220, and 358 MeV/u U^{92+} with N_2, CH_4, Ar, and Kr gaseous targets. For low-Z targets, the experimental REC data are found to be well described by exact relativistic calculations. Here, an application of the nonrelativistic dipole approximation, although theoretically not justified, also leads to a reasonable agreement with the experimental data. The NRC results, on the other hand, are well represented by the eikonal approach, except for high nuclear charges of the target system, where a slight deviation between experiment and theory is observed. However, in general, an overall agreement between experiment and theory can be stated. Therefore, the experimental data, together with the applied theoretical approach, can be used as a basis for estimates of beam losses at accelerator facilities when dealing with highly charged decelerated heavy ions and beam energies well above 10 MeV/u. For even lower energies, additional experimental studies are required in order to test the reliability of theoretical approaches. Only such investigations can decide the feasibility of experiments that require a deceleration to almost at rest. In particular, the luminosity available in such experiments is still unknown.

In order to deduce absolute cross-section values, we applied a technique that exploits x-ray radiation of REC into the K shell of the projectiles. Here we make use of the unprecedented clean and stable conditions of the ESR storage ring and we utilize the fact that differential REC cross sections are known to have a much higher precision than total reaction cross sections. Also state-selective and angular differential cross sections for all kinds of different reaction mechanisms can be determined by this method with a precision of a few percent.

A further improvement towards the 1% level of accuracy can be expected in the near future. With such an accuracy even the influence of quantum-electrodynamical effects on the dynamics of ion-atom encounters involving high-Z projectiles might be detectable. Besides magnetic and electron correlation effects, this will be one of the main topics of the next generation of experiments at the ESR gas-jet target where refined x-ray spectroscopy techniques will be applied. For this purpose a new target chamber has already been installed at the ESR gas-jet target which allows for angular differential collision studies, including observation angles from almost 0° to 180° as well as the application of x-ray/x-ray coincidence techniques.

ACKNOWLEDGMENTS

The work of three of us (P.S., Z.S., and A.W.) was supported by the State Committee of Scientific Research (Poland) under research Grant No. 2P03B10910 and by GSI in Darmstadt. R.W.D. was supported by GSI and the U.S. DOE, Office of Basic Energy Sciences. P.R. was supported by GSI and by the State Committee of Scientific Research (Poland) under Research Grant No. 2P30211907. The support by WTZ (P.M., T.S., Z.S., and A.W.) under Project No. POL-229-06 is acknowledged.

[1] R. Anholt and H. Gould, Adv. At. Mol. Phys. **22**, 315 (1986).
[2] J. Eichler, Phys. Rep. **193**, 165 (1990).
[3] J. Eichler and W. E. Meyerhof, *Relativistic Atomic Collisions* (Academic, San Diego, 1995).
[4] R. Anholt, W. E. Meyerhof, Ch. Stoller, E. Morenzoni, S. A. Andriamonje, J. D. Molitoris, O. K. Baker, D. H. H. Hoffmann, H. Bowman, J.-S. Xu, Z. Z. Xu, K. Frankel, D. Murphy, K. Crowe, and J. O. Rasmussen, Phys. Rev. A **30**, 2234 (1984).
[5] R. Anholt, Phys. Rev. A **31**, 3579 (1985).
[6] W. E. Meyerhof, R. Anholt, J. Eichler, H. Gould, Ch. Munger, J. Alonso, P. Thieberger, and H. E. Wegner, Phys. Rev. A **32**, 3291 (1985).
[7] R. Anholt, W. E. Meyerhof, H. Gould, Ch. Munger, J. Alonso, P. Thieberger, and H. E. Wegner, Phys. Rev. A **32**, 3302 (1985).
[8] R. Anholt, Ch. Stoller, J. D. Molitoris, D. W. Spooner, E. Morenzoni, S. A. Andriamonje, W. E. Meyerhof, H. Bowman, J.-S. Xu, Z.-Z. Xu, J. O. Rasmussen, and D. H. H. Hoffmann, Phys. Rev. A **33**, 2270 (1986).
[9] R. Anholt, W. E. Meyerhof, X.-Y. Xu, H. Gould, B. Feinberg, R. J. McDonald, H. E. Wegner, and P. Thieberger, Phys. Rev. A **36**, 1586 (1987).
[10] R. Anholt and U. Becker, Phys. Rev. A **36**, 4628 (1987).
[11] A. Belkacem, H. Gould, B. Feinberg, R. Bossingham, and W. E. Meyerhof, Phys. Rev. A **56**, 2806 (1997).
[12] C. R. Vane, S. Datz, E. F. Deveney, P. F. Dittner, H. F. Krause, R. Schuch, H. Gao, and R. Hutton, Phys. Rev. A **56**, 3682 (1997).
[13] H. F. Krause, C. R. Vane, S. Datz, P. Grafström, H. Knudsen, C. Scheidenberg, and R. Schuch, Phys. Rev. Lett. **80**, 1190 (1998).
[14] H. Reich, W. Bourgeois, B. Franzke, A. Kritzer, and V. Varentsov, Nucl. Phys. A **626**, 473c (1997).
[15] H. F. Beyer, G. Bollen, F. Bosch, P. Egelhof, B. Franzke, R. W. Hasse, H. J. Kluge, C. Kozhuharov, T. Kühl, D. Liesen, R. Mann, P. H. Mokler, A. Müller, R. W. Müller, G. Münzenberger, H. Poth, L. Schweikhard, R. Schuch, and G. Werth, GSI Report No. GSI-90-20, 1990.
[16] A. Gruber, W. Bourgeois, B. Franzke, A. Kritzer, and C. Treffert, Nucl. Instrum. Methods Phys. Res. A **282**, 87 (1989).
[17] Th. Stöhlker *et al.* (unpublished).
[18] Th. Stöhlker, C. Kozhuharov, P. H. Mokler, A. Warczak, F. Bosch, H. Geissel, R. Moshammer, C. Scheidenberger, J. Eichler, A. Ichihara, T. Shirai, Z. Stachura, and P. Rymuza, Phys. Rev. A **51**, 2098 (1995).
[19] P. H. Mokler and Th. Stöhlker, Adv. At. Mol. Phys. **37**, 297 (1996).
[20] G. Raisbeck and F. Yiou, Phys. Rev. Lett. **4**, 1858 (1971).
[21] H. W. Schnopper, H. Betz, J. P. Devaille, K. Kalata, A. R. Sohval, K. W. Jones, and H. E. Wegner, Phys. Rev. Lett. **29**, 898 (1972).
[22] P. Kienle, M. Kleber, B. Povh, R. M. Diamond, F. S. Stephens, E. Grosse, M. R. Maier, and D. Proetel, Phys. Rev. Lett. **31**, 1099 (1973).
[23] J. S. Briggs and K. Dettmann, Phys. Rev. Lett. **33**, 1123 (1974).
[24] M. Kleber and D. H. Jakubassa, Nucl. Phys. A **252**, 152 (1975).
[25] R. Shakeshaft and L. Spruch, Phys. Rev. Lett. **38**, 175 (1977).
[26] A. Ichihara, T. Shirai, and J. Eichler, Phys. Rev. A **49**, 1875 (1994).
[27] J. Eichler, A. Ichihara, and T. Shirai, Phys. Rev. A **51**, 3027 (1995).
[28] A. Ichihara, T. Shirai, and J. Eichler, Phys. Rev. A **54**, 4954 (1996).
[29] M. Stobbe, Ann. Phys. (Paris) **7**, 661 (1930).
[30] Th. Stöhlker, H. Geissel, H. Irnich, T. Kandler, C. Kozhuharov, P. H. Mokler, G. Münzenberg, F. Nickel, C. Scheidenberger, T. Suzuki, M. Kucharski, A. Warczak, P. Rymuza, Z. Stachura, A. Kriessbach, D. Dauvergene, B. Dunford, J. Eichler, A. Ichihara, and T. Shirai, Phys. Rev. Lett. **73**, 3520 (1994).
[31] Th. Stöhlker, C. Kozhuharov, P. H. Mokler, and A. Warczak, Comments At. Mol. Phys. **33**, 271 (1997).
[32] E. Clementi and C. Roetti, At. Data Nucl. Data Tables **14**, 177 (1974).
[33] A. Ichihara, T. Shirai, and J. Eichler, At. Data Nucl. Data Tables **55**, 63 (1993).
[34] Th. Stöhlker, P. H. Mokler, K. Beckert, F. Bosch, H. Eickhoff, B. Franzke, H. Geissel, M. Jung, T. Kandler, O. Klepper, C. Kozhuharov, R. Moshammer, F. Nickel, F. Nolden, H. Reich, P. Rymuza, C. Scheidenberger, P. Spädtke, Z. Stachura, M. Steck, and A. Warczak, Nucl. Instrum. Methods Phys. Res. B **87**, 64 (1994).
[35] P. Rymuza, Th. Stöhlker, H. Geissel, C. Kozhuharov, P. H. Mokler, R. Moshammer, F. Nickel, C. Scheidenberger, Z. Stachura, and A. Warczak, Acta Phys. Pol. B **27**, 573 (1996).
[36] J. Eichler, Phys. Rev. A **32**, 112 (1985).
[37] N. Toshima and J. Eichler, Phys. Rev. A **38**, 2305 (1988).
[38] H. Bethe and E. Salpeter, *Quantum Mechanics of One- and Two-Electron Systems*, Handbuch der Physik Vol. 57 (Springer, Berlin, 1957).